

involve

a journal of mathematics

The behavior of a population interaction-diffusion equation in
its subcritical regime

Mitchell G. Davis, David J. Wollkind,
Richard A. Cangelosi and Bonni J. Kealy-Dichone



The behavior of a population interaction-diffusion equation in its subcritical regime

Mitchell G. Davis, David J. Wollkind,
 Richard A. Cangelosi and Bonni J. Kealy-Dichone

(Communicated by Martin J. Bohner)

A model interaction-diffusion equation for population density originally analyzed through terms of third-order in its supercritical parameter range is extended through terms of fifth-order to examine the behavior in its subcritical regime. It is shown that under the proper conditions the two subcritical cases behave in exactly the same manner as the two supercritical ones unlike the outcome for the truncated system. Further, there also exists a region of metastability allowing for the possibility of population outbreaks. These results are then used to offer an explanation for the occurrence of isolated vegetative patches and sparse homogeneous distributions in the relevant ecological parameter range where there is subcriticality for a plant-groundwater model system, as opposed to periodic patterns and dense homogeneous distributions occurring in its supercritical regime.

1. Introduction and formulation of the problem

Consider the following interaction-diffusion partial differential equation boundary value problem for $N = N(s, \tau) \equiv$ population density, where $s \equiv$ one-dimensional spatial variable and $\tau \equiv$ time:

$$\frac{\partial N}{\partial \tau} = D_0 \frac{\partial^2 N}{\partial s^2} + R_0 N_e r \left(\frac{N - N_e}{N_e} \right), \quad 0 < s < L, \quad (1-1a)$$

$$N(0, \tau) = N(L, \tau) = N_e, \quad (1-1b)$$

with

$$r(\theta) = \theta + \alpha\theta^3 + \gamma\theta^5 + O(\theta^7). \quad (1-1c)$$

MSC2010: 34D20, 35Q56, 92D40.

Keywords: interaction-diffusion, Stuart–Watson method, subcritical bifurcation analysis.

Davis was supported by NSF 1029482 Collaborative Research: UBM-Institutional: UI-WSU Program in Undergraduate Mathematics and Biology.

Here, $D_0 \equiv$ dispersal constant, $R_0 \equiv$ interaction rate, $N_e \equiv$ equilibrium population density, and $L \equiv$ territory size, while α and γ represent dimensionless interaction coefficients. Note that

$$N(s, \tau) \equiv N_e \tag{1-2}$$

is an exact solution to boundary value problem (1-1).

Introducing the nondimensional variables and parameter

$$z = \frac{\pi s}{L}, \quad t = \frac{D_0 \pi^2 \tau}{L^2}, \quad \theta(z, t) = \frac{N(s, \tau) - N_e}{N_e}, \quad \beta = \frac{R_0 L^2}{D_0 \pi^2}, \tag{1-3}$$

our original problem transforms into

$$\frac{\partial \theta}{\partial t} - \frac{\partial^2 \theta}{\partial z^2} = \beta r(\theta), \quad 0 < z < \pi, \tag{1-4a}$$

$$\theta(0, t) = \theta(\pi, t) = 0. \tag{1-4b}$$

Note that the exact solution (1-2) to the dimensional problem corresponds to

$$\theta(z, t) \equiv 0 \tag{1-5}$$

for our dimensionless one (1-4).

This is an extension to fifth-order of a model equation introduced by Wollkind et al. [1994] to illustrate the Stuart–Watson method of weakly nonlinear stability analysis of prototype reaction-diffusion equations. Asymptotic analyses of this sort are very useful for predicting pattern formation in such nonlinear systems. That analysis requires the expansion of θ in powers of an unknown function $A(t)$ with spatially dependent coefficients. The pattern-formational aspect of this system can be predicted from the long-time behavior of that amplitude function, which is governed by its Landau ordinary differential equation

$$\frac{dA}{dt} \sim \sigma A - a_1 A^3 - a_3 A^5 = F(A), \tag{1-6}$$

where σ is the growth rate of linear stability theory and $a_{1,3}$ are the Landau constants. That long-time behavior is crucially dependent upon the signs of these Landau constants. Wollkind et al. [1994] concentrated on the special case for which $r(\theta) = \sin(\theta)$, employed by Matkowsky [1970] to develop his two-time method of weakly nonlinear stability theory, since their main concern was to compare the results obtained from the application of the Stuart–Watson method with those he deduced. Then $a_1 > 0$, identically (see below), and it is only necessary to include terms through third-order in $r(\theta)$ to make pattern formation predictions for this problem. In that event, there are two solutions of the truncated system: the first, a homogeneous one that is stable for $\sigma < 0$ and the second, a supercritical re-equilibrated pattern forming one that exists and is stable for $\sigma > 0$. These results

can be directly applied to our problem for its generalized $r(\theta)$ in the parameter range where $a_1 > 0$. In the range where $a_1 < 0$ and there is so-called subcriticality, the solutions to the truncated problem can grow without bound, and one must take the fifth-order terms into account in order to determine the long-time behavior of the system. Then we shall show that, if there is a parameter range over which the other Landau constant a_3 satisfies $a_3 > 0$, the pattern formation properties of our system can be ascertained without having to resort to considering even higher-order terms in $r(\theta)$. That requires the development of a formula for this Landau constant and an examination of its sign as a function of α and γ .

2. The Stuart–Watson method of nonlinear stability theory

Toward that end, we seek a Stuart–Watson expansion for the solution of our model equation of the form [Wollkind et al. 1994]

$$\begin{aligned} \theta(z, t) \sim A(t) \sin(z) + A^3(t)[\theta_{31} \sin(z) + \theta_{33} \sin(3z)] \\ + A^5(t)[\theta_{51} \sin(z) + \theta_{53} \sin(3z) + \theta_{55} \sin(5z)]. \end{aligned} \quad (2-1)$$

Note that the spatial terms in expansion (2-1) satisfy our boundary conditions (1-4b) at $z = 0$ and π , identically. Then, expanding $r(\theta)$ in powers of $A(t)$, employing the relevant trigonometric identities for the resulting products of sine functions contained in its coefficients, and making use of the Landau amplitude equation (1-6), we obtain a series of problems, one for each term appearing explicitly in our expansion of the form $A^n(t) \sin(mz)$, given by

$$\begin{aligned} A(t) \sin(z) : \quad \sigma + 1 &= \beta, \\ A^3(t) \sin(z) : \quad 3\sigma\theta_{31} - a_1 + \theta_{31} &= \beta(\theta_{31} + \frac{3}{4}\alpha), \\ A^3(t) \sin(3z) : \quad 3\sigma\theta_{33} + 9\theta_{33} &= \beta(\theta_{33} - \frac{1}{4}\alpha), \\ A^5(t) \sin(z) : \quad 5\sigma\theta_{51} - a_3 - 3a_1\theta_{31} + \theta_{51} &= \beta(\theta_{51} + \frac{9}{4}\alpha\theta_{31} - \frac{3}{4}\alpha\theta_{33} + \frac{5}{8}\gamma). \end{aligned}$$

Although there are also two other $A^5(t)$ problems, they have not been cataloged above since only the one proportional to $\sin(z)$ which involves a_3 is required for our purposes. Here, while σ and the θ_{nm} are being considered as functions of β , the coefficients $a_{1,3}$ are assumed to be independent of that bifurcation parameter and hence the use of the terminology Landau *constants*. That assumption is critical for their determination as solvability conditions, which is developed below.

We now solve these problems sequentially. Then, from the ones not involving these Landau constants, we obtain in a straightforward manner that

$$\sigma(\beta) = \beta - 1, \tag{2-2a}$$

and

$$\theta_{33}(\beta) = -\frac{\alpha\beta}{8(\beta+3)}, \quad (2-2b)$$

while the other two problems yield

$$2\sigma(\beta)\theta_{31}(\beta) = a_1 + \frac{3}{4}\alpha\beta \quad (2-2c)$$

and

$$4\sigma(\beta)\theta_{51}(\beta) = a_3 + 3\theta_{31}(\beta)\left(a_1 + \frac{3}{4}\alpha\beta\right) - \frac{3}{4}\alpha\beta\theta_{33}(\beta) + \frac{5}{8}\gamma\beta. \quad (2-2d)$$

(i) Assuming that $\theta_{31}(\beta)$ is well behaved at the critical bifurcation value of $\beta = 1$ and taking the limit of this first relation as $\beta \rightarrow 1$, while noting that $\sigma(\beta) = \beta - 1 \rightarrow 0$ in this limit, we obtain the solvability condition

$$a_1 = -\frac{3}{4}\alpha \quad (2-3a)$$

and, upon substitution of this back into (2-2c), the solution

$$\theta_{31}(\beta) \equiv \theta_{31} = \frac{3}{8}\alpha. \quad (2-3b)$$

Hence, we can deduce that

$$a_1 > 0 \quad \text{for } \alpha < 0 \quad \text{and} \quad a_1 < 0 \quad \text{for } \alpha > 0. \quad (2-4)$$

Thus, as mentioned earlier,

$$r(\theta) = \sin(\theta) = \theta - \frac{1}{6}\theta^3 + O(\theta^5) \implies \alpha = -\frac{1}{6} \implies a_1 = \frac{1}{8}. \quad (2-5)$$

Now, in this case, defining

$$\varepsilon^2 = \frac{\sigma(\beta)}{a_1} \quad \text{or} \quad \beta = 1 + \frac{1}{8}\varepsilon^2 \quad (2-6a)$$

and introducing the rescaled variables

$$\eta = \sigma t, \quad \mathcal{A}(\eta) = \frac{A(t)}{\varepsilon} \quad (2-6b)$$

into the truncated amplitude equation

$$\frac{d\mathcal{A}}{d\eta} = \sigma\mathcal{A} - a_1\mathcal{A}^3 + O(\mathcal{A}^5), \quad (2-6c)$$

we obtain

$$\frac{d\mathcal{A}}{d\eta} = \mathcal{A} - \mathcal{A}^3 + O(\varepsilon^2), \quad (2-6d)$$

which justifies that truncation procedure. Now multiplying the truncated amplitude equation by $A(t)$ and rewriting it as

$$\frac{1}{2} \frac{dA^2}{dt} = \sigma A^2 - a_1 A^4 = \sigma A^2 \left(1 - \frac{A^2}{\sigma/a_1}\right) = f_3(A^2), \quad (2-7)$$

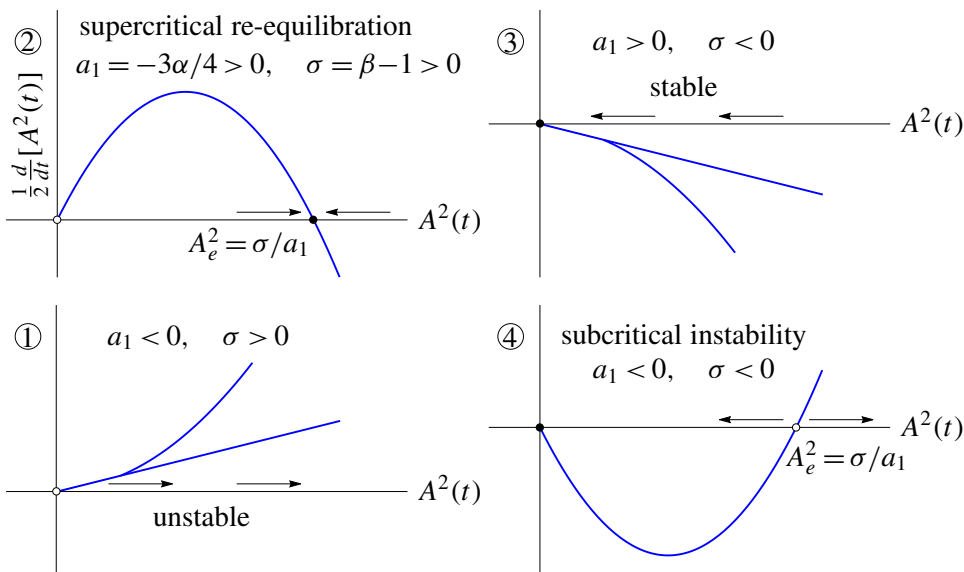


Figure 1. Plots of $f_3(A^2)$ for the third-order truncated amplitude equation with $\sigma = \beta - 1$ and $a_1 = -\frac{3}{4}\alpha$. Here the circled numbers correspond to the quadrants in the $\alpha\beta$ -space of Figure 5 with horizontal axis $\beta = 1$ and vertical axis $\alpha = 0$.

we can easily deduce its long-time behavior by means of the four phase-plane plots of

$$\frac{1}{2} \frac{dA^2}{dt} = f_3(A^2)$$

that constitute Figure 1, which catalogs the four qualitatively different cases corresponding to the possibility of σ and a_1 being either positive or negative. These serve as graphical representations of the cases discussed in Section 1 for the truncated version of our amplitude equation.

In particular, for the supercritical re-equilibration case of $\sigma, a_1 > 0$, we have

$$\lim_{t \rightarrow \infty} A(t) = A_e = \varepsilon, \tag{2-8a}$$

and hence

$$\lim_{t \rightarrow \infty} \theta(z, t) \sim \theta_e(z) = \delta \sin(z) \quad \text{as } \delta \rightarrow 0 \tag{2-8b}$$

since

$$\begin{aligned} \lim_{t \rightarrow \infty} \theta(z, t) &= \varepsilon \sin(z) + \varepsilon^3 [\theta_{31} \sin(z) + \theta_{33}(\beta) \sin(3z)] + O(\varepsilon^5) \\ &= (\varepsilon + \theta_{31}\varepsilon^3) \sin(z) + \varepsilon^3 \theta_{33}(1) \sin(3z) + O(\varepsilon^5) \\ &= \delta \sin(z) + \frac{1}{192} \delta^3 \sin(3z) + O(\delta^5) \sim \delta \sin(z) \quad \text{as } \delta \rightarrow 0, \end{aligned} \tag{2-8c}$$

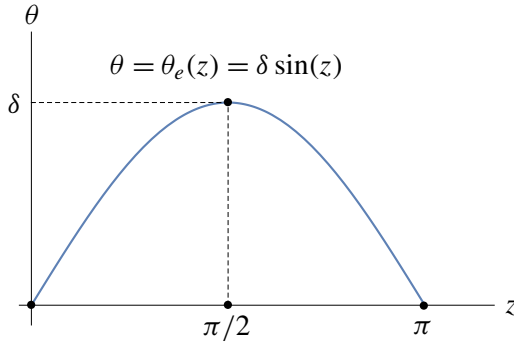


Figure 2. Plot of the arch solution $\theta_e(z)$ for $0 \leq z \leq \pi$.

where $\delta = \varepsilon + \varepsilon^3\theta_{31} > 0$. This equilibrium state, plotted in [Figure 2](#), is an arch-type pattern formed from one-cycle of a sine curve with its maximum amplitude δ occurring at $z = \frac{1}{2}\pi$.

(ii) We next proceed to analyze the second Landau constant relation [\(2-2d\)](#) involving a_3 and θ_{51} in an analogous manner to that just employed to evaluate a_1 and θ_{31} . Thus, assuming $\theta_{51}(\beta)$ to be well behaved at $\beta = 1$ and taking the limit of this relation as $\beta \rightarrow 1$, we obtain the solvability condition

$$a_3 = -\frac{5}{8}\gamma - 3\theta_{31}\left(a_1 + \frac{3}{4}\alpha\right) + \frac{3}{4}\alpha\theta_{33}(1) = -\frac{5}{8}\gamma - \frac{3}{128}\alpha^2 \tag{2-9a}$$

and, upon substitution of this back into [\(2-2d\)](#), the solution

$$\theta_{51}(\beta) = \frac{5}{32}\gamma + \frac{9}{16}\alpha\theta_{31} + \frac{3\alpha^2(4\beta + 3)}{512(\beta + 3)}. \tag{2-9b}$$

Observe that, by virtue of the value of a_1 , we have a_3 is independent of θ_{31} . Also observe that, unlike this quantity, θ_{51} is a function of β . Finally note, in addition, should we have assumed that the Stuart–Watson expansion for $\theta(z, t)$ and the Landau equation for dA/dt contained even powers of $A(t)$, then the solvability conditions and solutions for their coefficients would have shown them to be zero. Hence our implicit assumption that these quantities only contained odd powers was made without loss of generality and follows as a direct consequence of the form of $r(\theta)$.

Having determined its coefficients, we shall examine the truncated amplitude equation [\(1-6\)](#) through terms of fifth-order, i.e.,

$$\frac{dA}{dt} = F(A), \tag{2-10}$$

and defer until after this examination has been completed a justification for that truncation. We seek conditions under which the inclusion of fifth-order terms will re-equilibrate the growing solutions predicted through third-order when $a_1 < 0$. Hence we assume a parameter range in which $a_1 < 0$ or $\alpha > 0$. Further, anticipating

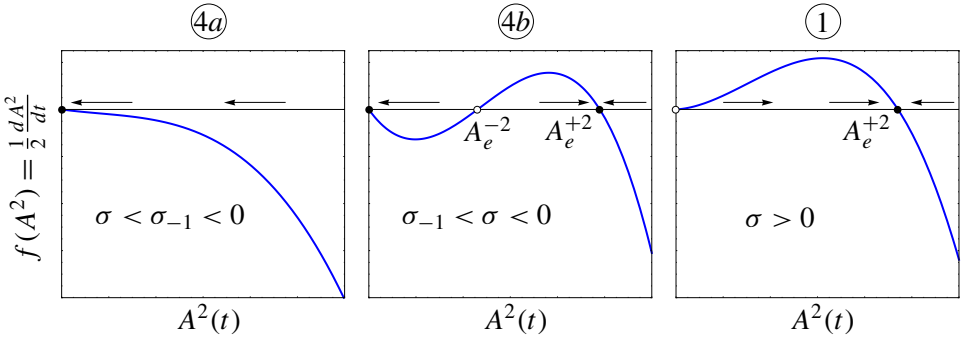


Figure 3. Plots of $f(A^2)$ for the fifth-order truncated amplitude equation with $a_1 < 0$; $a_3 > 0$; and $\sigma < \sigma_{-1} = -a_1^2/(4a_3) < 0$, $\sigma_{-1} < \sigma < 0$, and $\sigma > 0$, respectively. Here, the circled numbers correspond to the quadrants in the $\alpha\beta$ -space of [Figure 5](#).

our results to be demonstrated below, we assume that $a_3 > 0$, while, as always, $\sigma \in \mathbb{R}$. This equation has three equilibrium points

$$A(t) \equiv A_e \quad \text{such that } F(A_e) = 0 \quad (2-11a)$$

satisfying either

$$A_e = 0 \quad \text{or} \quad 2a_3 A_e^{\pm 2} = \pm \sqrt{a_1^2 + 4a_3 \sigma} - a_1. \quad (2-11b)$$

Observe that, since they must be real and positive, A_e^{+2} exists for $\sigma \geq \sigma_{-1} = -a_1^2/(4a_3)$, while A_e^{-2} only exists for $\sigma_{-1} \leq \sigma < 0$. Multiplying our truncated amplitude equation (2-10) by $A(t)$, we obtain

$$\frac{1}{2} \frac{dA^2}{dt} = \sigma A^2 - a_1 A^4 - a_3 A^6 = A^2 (A_e^{-2} - A^2)(A^2 - A_e^{+2}) = f(A^2). \quad (2-12)$$

Then we can determine the global stability properties of these equilibrium points by plotting $\frac{1}{2} dA^2/dt = f(A^2)$ for $\sigma < \sigma_{-1} < 0$, $\sigma_{-1} < \sigma < 0$, and $\sigma > 0$, respectively, in the three phase-plane plots of [Figure 3](#). From that figure, we can see that 0 is globally stable for $\sigma < \sigma_{-1} < 0$, A_e^{+2} is globally stable for $\sigma > 0$, and in the overlap region where either can be stable, depending on initial conditions, 0 is stable for $0 < A^2(0) < A_e^{-2}$ and A_e^{+2} is stable for $A^2(0) > A_e^{-2}$, while A_e^{-2} , which only exists in that bistability region, is not stable there.

To justify this truncation procedure we consider our Landau equation in the form

$$\frac{dA}{dt} = F(A) + O(A^7), \quad (2-13)$$

define $\varepsilon^2 = -a_1$, assume $a_3 = O(1)$ as $\varepsilon \rightarrow 0$, and let $\sigma = O(\varepsilon^4)$. Then $A_e^{+2} = O(\varepsilon^2)$, which implies that $A_e^+ = O(\varepsilon)$. Note, $\alpha = 10^{-2}$ and $\gamma = -2$ yield Landau constants

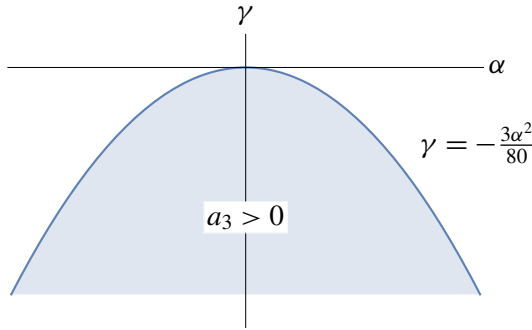


Figure 4. Plot of the region in the $\alpha\gamma$ -plane, where $a_3 > 0$.

satisfying these conditions. Now, analogous to our approach at third order, we introduce the rescaled variables

$$\eta = \sigma t, \quad \mathcal{A}(\eta) = A(t)/A_e^+, \quad \text{where } \mathcal{A}, \frac{d\mathcal{A}}{d\eta} = O(1) \text{ as } \varepsilon \rightarrow 0. \quad (2-14)$$

Since

$$\begin{aligned} \frac{dA}{dt} &= \sigma A_e^+ \frac{d\mathcal{A}}{d\eta} = O(\varepsilon^5), & \sigma A &= \sigma A_e^+ \mathcal{A} = O(\varepsilon^5), \\ a_1 A^3 &= a_1 A_e^+ \mathcal{A}^3 = O(\varepsilon^5), & a_3 A^5 &= a_3 A_e^+ \mathcal{A}^5 = O(\varepsilon^5), \end{aligned} \quad (2-15)$$

$$\text{while } O(A^7) = O(A_e^+ \mathcal{A}^7) = O(\varepsilon^7)$$

under these conditions, this justifies our truncation procedure at fifth order.

Finally, when $\sigma > 0$, we have the same type of equilibrium solution as depicted in Figure 2, except in this case

$$\delta = \varepsilon_0 + \theta_{31}(1)\varepsilon_0^3 + \theta_{51}(1)\varepsilon_0^5, \quad \text{where } A_e^+ = A_0\varepsilon = \varepsilon_0 \text{ with } A_0 = O(1) \text{ as } \varepsilon \rightarrow 0. \quad (2-16)$$

This result depends upon

$$a_3 > 0 \implies \gamma < -\frac{3}{80}\alpha^2. \quad (2-17)$$

Recall that, in addition, we have already taken $\alpha > 0$ to guarantee that $a_1 = -\frac{3}{4}\alpha < 0$. That region is plotted in the fourth quadrant of the $\alpha\gamma$ -plane of Figure 4. In this context, note from Figure 3 that, unlike the situation depicted in Figure 1 for $\alpha > 0$, all the solutions remain bounded when the fifth-order terms in $r(\theta)$ are retained.

3. Bifurcation diagram, ecological interpretations, and conclusions

Should there exist a parameter range in a dynamical systems model of a given phenomenon for which the third-order Landau constant a_1 satisfies $a_1 < 0$ and hence the bifurcation is subcritical, the weakly nonlinear stability analysis must

be pushed to fifth order as originally pointed out by DiPrima et al. [1971]. This has been standard operating procedure particularly over the last five years when practitioners of the Palermo nonlinear stability theory group began considering fifth-order terms in the Landau equation during their investigation of subcritical bifurcation for a variety of two-component reaction-diffusion systems [Gambino et al. 2010; 2012; Tulumello et al. 2014]. By necessity, such calculations are long and technically complicated. Thus, when surveying the theory, there is some merit in introducing a simple model equation that preserves all the salient features of a more complex system but considerably reduces the labor involved in determining the Landau constants. This was our rationale for considering the generalized Matkowsky equation under investigation. That was also the rationale for Drazin and Reid's [1981] employment of their nondimensionalized version of the Matkowsky equation in order to develop weakly nonlinear theory relevant to hydrodynamic stability. Matkowsky [1970] regarded his problem as a mathematical model for temperature distribution in a finite bar with a nonlinear source term, the ends of which were maintained at the ambient, while Drazin and Reid [1981] offered their corresponding version as a phenomenological model of parallel flow in a channel. Hence, they both envisioned their instabilities to be rate-driven by considering the bifurcation parameter $\beta \sim R_0$. For ecological applications, it is often more relevant to envision these instabilities to be *territory-size* driven by considering $\beta \sim L^2$ and then the instability criterion describes the evolution of spatially heterogeneous structure in a specific domain.

Given that the fifth-order extensions referenced above primarily concentrated only on the subcritical regime, we begin this section by synthesizing our fifth-order results of Figure 3 valid for $a_1 < 0$ or, equivalently, $\alpha > 0$, and $a_3 > 0$ or, equivalently, $3\alpha^2 + 80\gamma < 0$, with those valid for $a_1 > 0$ or, equivalently, $\alpha < 0$, and $a_3 > 0$, as well. Note, that under these conditions, $A_e^{+2} > 0$ for $\sigma > 0$ and $A_e^{-2} < 0$, identically. If we plot a figure analogous to the supercritical cases of Figure 1, it is obvious that the qualitative morphological behavior of those cases is preserved at fifth order with the only change being now $A_e^2 = A_e^{+2}$. We accomplish this synthesis by means of Figure 5, a bifurcation diagram in $\alpha\beta$ -space, where the relevant regions associated with these predicted morphological identifications are represented graphically. Since those results also depend on the behavior of σ , while $\sigma = 0$ and $\sigma = \sigma_{-1}$ are the critical loci for that quantity in this regard, it is necessary for us to generate loci equivalent to them in $\alpha\beta$ -space. In this context, using our previous solvability conditions and definitions, we can deduce the following equivalences:

$$\begin{aligned} \sigma = \beta - 1 = 0 & \iff \beta = 1, \\ \sigma = \beta - 1 = \sigma_{-1} = -\frac{a_1^2}{4a_3} = \frac{18\alpha^2}{3\alpha^2 + 80\gamma} & \iff \beta = 1 + \frac{18\alpha^2}{3\alpha^2 + 80\gamma}, \end{aligned} \quad (3-1)$$

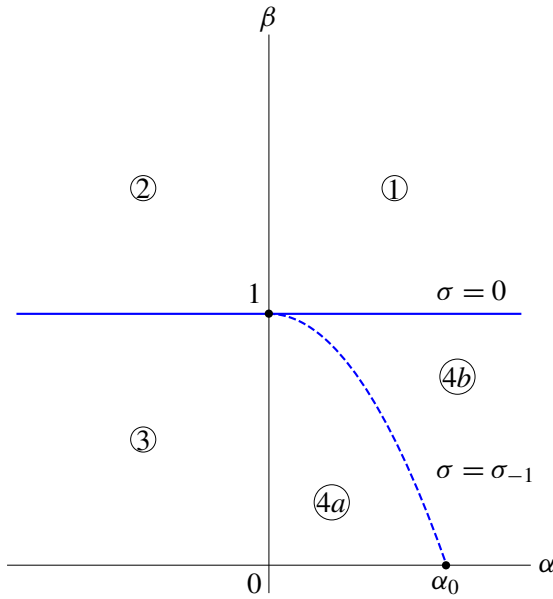


Figure 5. Bifurcation diagram in $\alpha\beta$ -space with $\sigma_{-1} = -a_1^2/(4a_3)$, $\sigma = \beta - 1$, $a_1 = -\frac{3}{4}\alpha$, and $a_3 = -\frac{5}{8}\gamma - \frac{3}{128}\alpha^2 > 0$, where the circled numbers correspond to the quadrants denoted in Figures 1 and 3.

quadrant	1	2	3	4a	4b
stable equilibrium point	A_e^{+2}	A_e^{+2}	0	0	$\begin{matrix} 0 \\ A_e^{+2} \end{matrix}$

Table 1. Stable equilibrium points for A^2 in the quadrants of Figure 5.

which are plotted in Figure 5. Here, that first locus is a horizontal line parallel to the α -axis which divides our $\alpha\beta$ -space into the four quadrants formed by it and the β -axis, while the second is a concave downward decreasing curve having a horizontal tangent at its β -intercept of 1 and an α -intercept of $\alpha_0 > 0$, where $\alpha_0^2 = -\frac{80}{21}\gamma$, which separates the fourth quadrant of that space into two parts. From an examination of the modification of the supercritical cases of Figure 1 described above and the subcritical cases of Figure 3, we construct Table 1 cataloging the stable equilibrium points for A^2 in each of the quadrants of Figure 5.

Note that these fifth-order results for our model equation are much more self-consistent than those obtained in the case of its third-order truncation, in that, the behavior for the subcritical quadrants 1 and 4a now exactly resemble the behavior for the supercritical quadrants 2 and 3, respectively. In the subcritical quadrant 4b, we have what biologists refer to as metastability, in that, the 0 equilibrium point is

quadrant	1	2	3	4a	4b
stable pattern	arch	arch	dense hom.	sparse hom.	sparse hom. arch

Table 2. Morphological stability predictions for [Table 1](#).

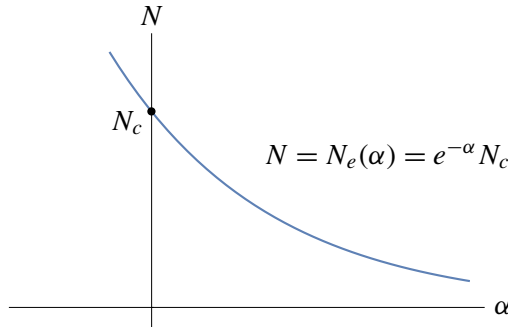


Figure 6. Plot of the population equilibrium density N_e versus α .

stable to initially small disturbances, but the model will switch to the equilibrium point A_e^{+2} for sufficiently large ones. The existence of such a region of metastability allows our model equation to exhibit outbreak behavior wherein the maximum population level increases several-fold upon a sufficient initial perturbation in amplitude.

Returning to our original dimensional formulation (1-1), the fact that $A^2 = 0$ represents a globally stable equilibrium point implies that

$$\lim_{\tau \rightarrow \infty} N(s, \tau) = N_e. \tag{3-2}$$

Hence this solution represents a homogeneous population. In many actual biological systems, such as the interaction-diffusion plant-groundwater one employed by Chaiya et al. [2015] to model vegetative pattern formation in a flat arid environment, the homogeneous patterns in the subcritical parameter range correspond to relatively sparse distributions, while most of those patterns in the supercritical range correspond to much denser distributions, where the threshold between these two types of distributions occurs at some N_c . We can induce this sort of behavior in our model equation by adopting the relationship

$$N_e = N_e(\alpha) = N_c e^{-\alpha}, \tag{3-3}$$

which is plotted in [Figure 6](#). Then from this relation and [Table 1](#) in conjunction with [Figure 2](#), we can deduce the stable pattern predictions given in [Table 2](#) for the quadrants of [Figure 5](#).

In [Chaiya et al. 2015], it was conjectured that the region of parameter space of subcriticality, where $a_1 < 0$, corresponded to isolated vegetative patches when $\sigma > 0$ and low-density homogeneous distributions when $\sigma < 0$, as opposed to the occurrence of periodic patterns for $\sigma > 0$ and high-density homogeneous distributions when $\sigma < 0$, where $a_1 > 0$, which were already predicted by their rhombic-planform two-dimensional nonlinear stability analysis. Such isolated patches are a compromise between periodic patterns and homogeneous stable states that are sparse enough to resemble bare ground. They then associated equilibrium points 0 and A_e^{+2} of quadrants 1 and 4 of Table 1 with the sparse homogeneous state and the isolated patch, respectively, that would occur in a postulated fifth-order extension, should $a_3 > 0$ for this parameter range. Our fifth-order results summarized in Table 2 represent the first step in a conclusive demonstration of the validity of this conjecture.

We conclude by noting that although these results are only strictly asymptotically valid in a neighborhood of the marginal stability curve $\beta = 1$, Boonkorkuea et al. [2010], by comparing their theoretical predictions of this sort with existing numerical simulations of vegetative pattern formation for a model evolution equation, recently showed that the former can often be extrapolated to those regions of parameter space relatively far from the marginal curve. These theoretical predictions also associated that region of parameter space, where numerical simulation generated isolated patches, with $\sigma > 0$ and $a_1 < 0$.

Finally, we close by offering, for the sake of definiteness, a closed-form representation of $r(\theta)$, composed of combinations of common functions that produce Landau constants consistent in sign with our subcriticality assumptions. Recall the following Maclaurin polynomials truncated through terms of fifth order:

$$\sinh(z) \sim z + \frac{1}{6}z^3 + \frac{1}{120}z^5 \quad \text{and} \quad \arctan(z) \sim z - \frac{1}{3}z^3 + \frac{1}{5}z^5. \quad (3-4)$$

Then

$$\begin{aligned} 4 \sinh\left(\frac{1}{2}\theta\right) &\sim 4\left(\frac{1}{2}\theta + \frac{1}{48}\theta^3 + \frac{1}{3840}\theta^5\right) = 2\theta + \frac{1}{12}\theta^3 + \frac{1}{960}\theta^5, \\ 2 \arctan\left(\frac{1}{2}\theta\right) &\sim 2\left(\frac{1}{2}\theta - \frac{1}{24}\theta^3 + \frac{1}{160}\theta^5\right) = \theta - \frac{1}{12}\theta^3 + \frac{1}{80}\theta^5. \end{aligned} \quad (3-5)$$

Now, defining $r(\theta)$ to be the difference between these two functions, we obtain

$$\alpha = \frac{1}{6} > 0, \quad \gamma = -\frac{11}{960} \quad \text{such that} \quad 80\gamma + 3\alpha^2 = -\frac{11}{12} + \frac{1}{12} = -\frac{5}{6} < 0. \quad (3-6)$$

References

- [Boonkorkuea et al. 2010] N. Boonkorkuea, Y. Lenbury, F. J. Alvarado, and D. J. Wollkind, “Nonlinear stability analyses of vegetative pattern formation in an arid environment”, *J. Biol. Dyn.* **4:4** (2010), 346–380. MR Zbl
- [Chaiya et al. 2015] I. Chaiya, D. J. Wollkind, R. A. Cangelosi, B. J. Kealy-Dichone, and C. Ratanakul, “Vegetative rhombic pattern formation driven by root suction for an interaction-diffusion

plant-ground water model system in an arid flat environment”, *Amer. J. Plant Sci.* **6**:8 (2015), 1278–1300.

- [DiPrima et al. 1971] R. C. DiPrima, W. Eckhaus, and L. A. Segel, “Non-linear wave-number interaction in near-critical two-dimensional flows”, *J. Fluid Mech.* **49**:4 (1971), 705–744. [Zbl](#)
- [Drazin and Reid 1981] P. G. Drazin and W. H. Reid, *Hydrodynamic stability*, Cambridge Univ. Press, 1981. [MR](#) [Zbl](#)
- [Gambino et al. 2010] G. Gambino, A. M. Greco, M. C. Lombardo, and M. Sammartino, “A subcritical bifurcation for a nonlinear reaction-diffusion system”, pp. 163–172 in *Waves and stability in continuous media* (Palermo, 2009), edited by A. M. Greco et al., World Sci. Publ., Hackensack, NJ, 2010. [MR](#) [Zbl](#)
- [Gambino et al. 2012] G. Gambino, M. C. Lombardo, and M. Sammartino, “Turing instability and traveling fronts for a nonlinear reaction-diffusion system with cross-diffusion”, *Math. Comput. Simulation* **82**:6 (2012), 1112–1132. [MR](#) [Zbl](#)
- [Matkowsky 1970] B. J. Matkowsky, “A simple nonlinear dynamic stability problem”, *Bull. Amer. Math. Soc.* **76** (1970), 620–625. [MR](#) [Zbl](#)
- [Tulumello et al. 2014] E. Tulumello, M. C. Lombardo, and M. Sammartino, “Cross-diffusion driven instability in a predator-prey system with cross-diffusion”, *Acta Appl. Math.* **132** (2014), 621–633. [MR](#) [Zbl](#)
- [Wollkind et al. 1994] D. J. Wollkind, V. S. Manoranjan, and L. Zhang, “Weakly nonlinear stability analyses of prototype reaction-diffusion model equations”, *SIAM Rev.* **36**:2 (1994), 176–214. [MR](#) [Zbl](#)

Received: 2016-10-15

Revised: 2017-01-27

Accepted: 2017-02-04

m.g.davis@outlook.com

*Department of Mathematics, Washington State University,
Pullman, WA, United States*

dwoollkind@wsu.edu

*Department of Mathematics, Washington State University,
Pullman, WA, United States*

cangelosi@gonzaga.edu

*Department of Mathematics, Gonzaga University,
Spokane, WA, United States*

dichone@gonzaga.edu

*Department of Mathematics, Gonzaga University,
Spokane, WA, United States*

INVOLVE YOUR STUDENTS IN RESEARCH

Involve showcases and encourages high-quality mathematical research involving students from all academic levels. The editorial board consists of mathematical scientists committed to nurturing student participation in research. Bridging the gap between the extremes of purely undergraduate research journals and mainstream research journals, *Involve* provides a venue to mathematicians wishing to encourage the creative involvement of students.

MANAGING EDITOR

Kenneth S. Berenhaut Wake Forest University, USA

BOARD OF EDITORS

Colin Adams	Williams College, USA	Suzanne Lenhart	University of Tennessee, USA
John V. Baxley	Wake Forest University, NC, USA	Chi-Kwong Li	College of William and Mary, USA
Arthur T. Benjamin	Harvey Mudd College, USA	Robert B. Lund	Clemson University, USA
Martin Bohner	Missouri U of Science and Technology, USA	Gaven J. Martin	Massey University, New Zealand
Nigel Boston	University of Wisconsin, USA	Mary Meyer	Colorado State University, USA
Amarjit S. Budhiraja	U of North Carolina, Chapel Hill, USA	Emil Minchev	Ruse, Bulgaria
Pietro Cerone	La Trobe University, Australia	Frank Morgan	Williams College, USA
Scott Chapman	Sam Houston State University, USA	Mohammad Sal Moslehian	Ferdowsi University of Mashhad, Iran
Joshua N. Cooper	University of South Carolina, USA	Zuhair Nashed	University of Central Florida, USA
Jem N. Corcoran	University of Colorado, USA	Ken Ono	Emory University, USA
Toka Diagana	Howard University, USA	Timothy E. O'Brien	Loyola University Chicago, USA
Michael Dorff	Brigham Young University, USA	Joseph O'Rourke	Smith College, USA
Sever S. Dragomir	Victoria University, Australia	Yuval Peres	Microsoft Research, USA
Behrouz Emamizadeh	The Petroleum Institute, UAE	Y.-F. S. Pétermann	Université de Genève, Switzerland
Joel Foisy	SUNY Potsdam, USA	Robert J. Plemmons	Wake Forest University, USA
Erin W. Fulp	Wake Forest University, USA	Carl B. Pomerance	Dartmouth College, USA
Joseph Gallian	University of Minnesota Duluth, USA	Vadim Ponomarenko	San Diego State University, USA
Stephan R. Garcia	Pomona College, USA	Bjorn Poonen	UC Berkeley, USA
Anant Godbole	East Tennessee State University, USA	James Propp	U Mass Lowell, USA
Ron Gould	Emory University, USA	József H. Przytycki	George Washington University, USA
Andrew Granville	Université Montréal, Canada	Richard Rebarber	University of Nebraska, USA
Jerrold Griggs	University of South Carolina, USA	Robert W. Robinson	University of Georgia, USA
Sat Gupta	U of North Carolina, Greensboro, USA	Filip Saidak	U of North Carolina, Greensboro, USA
Jim Haglund	University of Pennsylvania, USA	James A. Sellers	Penn State University, USA
Johnny Henderson	Baylor University, USA	Andrew J. Sterge	Honorary Editor
Jim Hoste	Pitzer College, USA	Ann Trenk	Wellesley College, USA
Natalia Hritonenko	Prairie View A&M University, USA	Ravi Vakil	Stanford University, USA
Glenn H. Hurlbert	Arizona State University, USA	Antonia Vecchio	Consiglio Nazionale delle Ricerche, Italy
Charles R. Johnson	College of William and Mary, USA	Ram U. Verma	University of Toledo, USA
K. B. Kulasekera	Clemson University, USA	John C. Wierman	Johns Hopkins University, USA
Gerry Ladas	University of Rhode Island, USA	Michael E. Zieve	University of Michigan, USA

PRODUCTION

Silvio Levy, Scientific Editor


Cover: Alex Scorpan

See inside back cover or msp.org/involve for submission instructions. The subscription price for 2018 is US \$190/year for the electronic version, and \$250/year (+\$35, if shipping outside the US) for print and electronic. Subscriptions, requests for back issues and changes of subscriber address should be sent to MSP.

Involve (ISSN 1944-4184 electronic, 1944-4176 printed) at Mathematical Sciences Publishers, 798 Evans Hall #3840, c/o University of California, Berkeley, CA 94720-3840, is published continuously online. Periodical rate postage paid at Berkeley, CA 94704, and additional mailing offices.

Involve peer review and production are managed by EditFLOW® from Mathematical Sciences Publishers.

PUBLISHED BY

 **mathematical sciences publishers**
nonprofit scientific publishing

<http://msp.org/>

© 2018 Mathematical Sciences Publishers

involve

2018

vol. 11

no. 2

Finding cycles in the k -th power digraphs over the integers modulo a prime	181
GREG DRESDEN AND WENDA TU	
Enumerating spherical n -links	195
MADELEINE BURKHART AND JOEL FOISY	
Double bubbles in hyperbolic surfaces	207
WYATT BOYER, BRYAN BROWN, ALYSSA LOVING AND SARAH TAMMEN	
What is odd about binary Parseval frames?	219
ZACHERY J. BAKER, BERNHARD G. BODMANN, MICAH G. BULLOCK, SAMANTHA N. BRANUM AND JACOB E. MCLANEY	
Numbers and the heights of their happiness	235
MAY MEI AND ANDREW READ-MCFARLAND	
The truncated and supplemented Pascal matrix and applications	243
MICHAEL HUA, STEVEN B. DAMELIN, JEFFREY SUN AND MINGCHAO YU	
Hexatonic systems and dual groups in mathematical music theory	253
CAMERON BERRY AND THOMAS M. FIORE	
On computable classes of equidistant sets: finite focal sets	271
CSABA VINCZE, ADRIENN VARGA, MÁRK OLÁH, LÁSZLÓ FÓRIÁN AND SÁNDOR LŐRINC	
Zero divisor graphs of commutative graded rings	283
KATHERINE COOPER AND BRIAN JOHNSON	
The behavior of a population interaction-diffusion equation in its subcritical regime	297
MITCHELL G. DAVIS, DAVID J. WOLLKIND, RICHARD A. CANGELOSI AND BONNI J. KEALY-DICHONE	
Forbidden subgraphs of coloring graphs	311
FRANCISCO ALVARADO, ASHLEY BUTTS, LAUREN FARQUHAR AND HEATHER M. RUSSELL	
Computing indicators of Radford algebras	325
HAO HU, XINYI HU, LINHONG WANG AND XINGTING WANG	
Unlinking numbers of links with crossing number 10	335
LAVINIA BULAI	
On a connection between local rings and their associated graded algebras	355
JUSTIN HOFFMEIER AND JIYOON LEE	